FICD acts bi-functionally to AMPylate and de-AMPylate the endoplasmic reticulum chaperone BiP

Steffen Preissler[#1,*], **Claudia Rato**[#1], **Luke Perera**[1], **Vladimir Saudek**[2], and **David Ron**[1,*]

[1]Cambridge Institute for Medical Research, University of Cambridge, Cambridge, United Kingdom

[2]Institute of Metabolic Science, University of Cambridge, Cambridge, United Kingdom

[#] These authors contributed equally to this work.

Abstract

Protein folding homeostasis in the endoplasmic reticulum (ER) is defended by an unfolded protein response (UPR) that matches ER chaperone capacity to the burden of unfolded proteins. As levels of unfolded proteins decline, a metazoan-specific FIC-domain containing ER-localized enzyme, FICD (HYPE), rapidly inactivates the major ER chaperone BiP by AMPylating T518. Here we show that the single catalytic domain of FICD can also release the attached AMP, restoring functionality to BiP. Consistent with a role for endogenous FICD in de-AMPylating BiP, *FICD*^{-/-} hamster cells are hypersensitive to introduction of a constitutively AMPylating, de-AMPylation defective mutant FICD. These opposing activities hinge on a regulatory residue, E234, whose default state renders FICD a constitutive de-AMPylase in vitro. The location of E234 on a conserved regulatory helix and the mutually antagonistic activities of FICD in vivo, suggest a mechanism whereby fluctuating unfolded protein load actively switches FICD from a de-AMPylase to an AMPylase.

Introduction

The balance of chaperones and unfolded proteins in the endoplasmic reticulum (ER) is important to the functionality and health of all secretory cells and affects the outcome of diverse protein misfolding and aging-related diseases 1,2. Conserved transcriptional and translational mechanisms, operative on a timescale of hours, match ER folding capacity to client protein abundance in all eukaryotes 3. In metazoans this unfolded protein response

(UPR) is complemented by processes that rapidly inactivate and reactivate the ER-localized Hsp70 chaperone BiP to match fluctuating levels of unfolded proteins during the inherent delay of the UPR.

Two processes are known to contribute to this short-term post-transcriptional buffering. Firstly, client protein binding is in competition with rapid self-binding of BiP to form oligomers that serve as a pool of recruitable inactive chaperone [4–6]. Secondly, an enzymatically-mediated inactivating covalent modification of BiP, which is conspicuous when unfolded proteins are scarce [7,8] functions alongside mass-action mediated oligomerization to match BiP activity to client protein load. Long believed to be ADP-ribosylation [4,9], this modification is now known to be AMPylation [10–12]; the covalent attachment of adenosine monophosphate (AMP), via a phosphodiester bond to the hydroxyl side chain of a residue in the target protein (also known as adenylylation) [13].

The ER-localized FIC- (filamentation induced by cyclic AMP) domain containing protein, FICD (HYPE) [14], uses ATP to AMPylate BiP both in vitro and in vivo [10–12,15]. In cultured mammalian cells, deletion of the *FICD* gene abolishes all evidence for BiP modification, which is otherwise observed at high stoichiometry on threonine 518. AMPylated BiP (BiP$^{T518-AMP}$) is only weakly stimulated by J-domain proteins and the modified chaperone is locked in a relatively inert state [12]. Like other FIC enzymes FICD's AMPylation activity is intrinsically repressed by the intra-molecular engagement of regulatory residue, glutamate 234, in FICD's active site [16,17]. However, enforced expression of a constitutive AMPylating FICD mutant (that bypasses the aforementioned intrinsic repressive mechanism) results in high levels of ER stress – most likely a consequence of BiP inactivation. These genetic and biochemical findings point to FICD as being both necessary and sufficient for BiP AMPylation observed when the burden of unfolded ER proteins is low.

As unfolded proteins accumulate, pre-existing AMPylated BiP is rapidly converted to the active de-AMPylated state [6,11,12], indicating that BiP AMPylation is a reversible modification that contributes to the balance between clients and chaperone in the ER. Regulatory, de-AMPylating enzymes are known to exist: AMPylated *E. coli* glutamine synthetase is reactivated by a de-AMPylase encoded by the N-terminal portion of the same polypeptide that also encodes the AMPylase [18,19], whereas in the course of *L. pneumophilia* infection, the AMPylated, inactivated mammalian host GTPase Rab1 is reactivated by a bacterially-encoded de-AMPylating enzyme, SidD [20]. However, the counterparts to such enzymes in the mammalian ER are not obvious. This study therefore addresses the hitherto mysterious process by which the phosphodiester bond between AMP and the hydroxyl side chain of BiP's T518 is broken and full BiP chaperone activity restored.

Results

Overexpression of wildtype FICD cannot restore BiP AMPylation in FICD-deficient cells

AMPylated BiP, detected by its characteristic mobility on native-PAGE or in isoelectric focusing gels, is readily observed upon inhibition of protein synthesis in wildtype but not

FICD^{-/-} cells (Fig. 1). However, overexpression of FICD fails to restore AMPylation to *FICD*^{-/-} cells. ER stress caused by FICD overexpression, is unlikely to contribute to the lack of AMPylated BiP as UPR signaling was not activated in the transfected cells (see below). By contrast, the hyperactive allele FICD[E234G] readily restored AMPylated BiP in *FICD*^{-/-} cells [Fig. 1, lanes 4 & 5 and Fig. 2D in reference 12].

Unlike the transfected wildtype FICD, neither the endogenous FICD, nor the hyperactive FICD[E234G] are reliably detectable in our immunoblots. This consistent finding reflects the low abundance of endogenous FICD in cells 12 and indicates that, though greatly overexpressed, the wildtype enzyme is unable to promote AMPylated BiP in *FICD*^{-/-} cells. This finding suggested the possibility that levels of AMPylated BiP are biphasically-related to the concentration of wildtype FICD (but not mutant FICD[E234G]) and that in addition to AMPylating BiP, wildtype FICD also has a role in undoing the modification; a function that dominates in overexpression-prone *trans*-rescue experiments.

FICD de-AMPylates BiP in vitro

Speculation that failure to rescue AMPylation reflects narrow tolerance for FICD dosage effects consequent to opposing actions of a single FICD enzyme is further supported by observations that AMPylation and de-AMPylation of bacterial glutamine synthetase is carried out by two structurally-related nucleotidylyl transferase-like domains on the same polypeptide 19. Whilst the active sites of the aforementioned Glutamine Synthetase Adenylyl Transferase (GS-ATase) are not obviously related to FIC, the FIC fold also flexibly catalyzes diverse phospho-transfer reactions 21–23. Therefore, it seemed reasonable to examine the ability of FICD to remove the AMP moiety from BiP[T518-AMP].

The signal arising from the ^{32}P-labeled AMP of purified BiP[T518-AMP] is very stable, with negligible rates of spontaneous hydrolysis. However, addition of wildtype FICD led to a time-dependent decrease in radiolabel; a feature shared neither by the AMPylation-competent, hyperactive FICD[E234G] nor by the AMPylation-defective FICD[H363A] mutant enzyme (Fig. 2a). These de-AMPylation reactions were performed in the absence of ATP, precluding re-AMPylation by any residual hyperactive AMPylating FICD[E234G] (carried over from the preceding AMPylation reaction). The de-AMPylating activity of wildtype FICD was not restricted to recombinant BiP AMPylated *in vitro*, as incubating lysates from cycloheximide-treated cells with pure wildtype FICD also led to disappearance of the acidic AMPylated form of endogenous BiP, as revealed by isoelectric focusing (Fig. 2b).

Wildtype FICD's ability to catalyze the removal of AMP from BiP[T518-AMP] was confirmed kinetically by following the decline in the fluorescence polarization signal arising from BiP AMPylated in vitro with fluorescent ATP-FAM as a substrate (BiP[T518-AMP-FAM]; Supplementary Fig. 1). Importantly, various substitutions of FICD[E234] generated mutant enzymes with widely different constitutive AMPylating activities (Fig. 2c), however, all lacked detectable de-AMPylating activity (Fig. 2d), attesting to the dual role of this residue in regulating AMPylation 16,17 and in affecting de-AMPylation.

FICD-mediated de-AMPylation products

To further characterize the FICD-mediated de-AMPylation reaction its products were analyzed. Comparison of the native mass of unmodified and modified BiP, whether from FICD-containing cells or from samples reacted with FICD and ATP in vitro, point to the addition of a single AMP moiety on any given molecule of BiP 12. Liquid chromatography coupled to mass spectrometry (LC-MS) of peptides arising from a digest with Arg-C proteinase revealed the presence of a single mono-AMPylated BiP[511-532] peptide [m/z= 1375.15 (2+)] 12 that was absent from samples of BiP that had never been AMPylated [12 and Fig. 3a, upper panel]. Crucially, this signal was abolished by exposure to wildtype FICD but not by exposure to the FICD[H363A] mutant (Fig. 3a, middle and lower panels). The loss of the AMPylated BiP[511-532] peptide caused by FICD was matched by gain in peptides with the mass of the unmodified BiP[511-532] [m/z= 1209.62 (2+)] (Fig. 3b) pointing to the ability of FICD to revert BiP[T518-AMP] to its pre-modified state.

To examine the fate of the modifying nucleotide, protein-free supernatants of in vitro de-AMPylation reactions were examined by ion pair chromatography. Exposure of BiP[T518-AMP] to wildtype FICD led to the emergence of a 254 nm absorbance peak that overlapped with the AMP marker (Fig. 3c, red trace) and had indistinguishable absorption spectra by three-dimensional analysis (Supplementary Fig. 2). The AMP peak was conspicuously absent from reactions set up with wildtype FICD and non-AMPylated BiP (green trace) or AMPylated BiP and the inactive FICD[H363A] mutant (blue trace). These experiments point to a role of FICD as a phosphodiesterase that liberates AMP from AMPylated BiP.

AMPylated BiP is locked into a low-substrate affinity, interdomain-coupled state that is relatively resistant to cleavage by SubA 12, a highly specific protease that cuts the interdomain linker of BiP 24. Native-PAGE revealed that exposure to wildtype FICD imparted sensitivity to SubA on AMPylated BiP (Fig. 3d). In the absence of ATP, BiP forms higher order oligomers, a process that is impeded by AMPylation 6. Exposure to wildtype FICD led to oligomerization of the largely monomeric AMPylated form of BiP (Fig. 3e, compare lanes 3 & 4). The FICD-mediated conversion of modified BiP to self-binding unmodified BiP was also noticeable in native gels of samples in presence of ATP; but only BiP dimers were detectable (Fig. 3d, compare lanes 1 & 2). Thus, FICD restored BiP to its pre-AMPylated functional state.

Enzymatic properties of the FICD de-AMPylase

FICD-mediated BiP AMPylation is specific for the intact full-length BiP as the enzyme fails to recognize T518 when the latter is presented in the context of the isolated substrate-binding domain of BiP 12. To examine the substrate specificity of FICD's phosphodiesterase activity, the ability of SubA to cleave AMPylated BiP quantitatively (by prolonged incubation) was exploited. Exposure to FICD led to the time-dependent disappearance of the fluorescent signal from intact BiP[T518-AMP-FAM]. However, FICD was unable to remove the fluorescent moiety from the isolated substrate-binding domain of BiP[T518-AMP-FAM] (Fig. 4a).

Kinetic analysis of FICD's phosphodiesterase activity revealed the expected enzyme concentration-dependence of the reaction (Fig. 4b) and a substrate K_M of 15.58 ± 3.27 μM and a k_{cat} of $9.89 \pm 0.87 \times 10^{-3}$ sec^{-1} (Fig. 4c). These observations are consistent with a specific but relatively slow de-AMPylase, sensitive to the lower end of physiological fluctuations predicted in the concentration of its substrate. Given that BiP de-AMPylation proceeds in the absence of co-factors or activators, these in vitro observations are consistent with the idea that overexpression of wildtype FICD exposes the ER to high levels of a protein whose default activity is to de-AMPylation BiP.

Glu234 switches FICD from AMPylation to de-AMPylation

The FICD-mediated BiP AMPylation/de-AMPylation cycle converts the co-substrate ATP to AMP and pyrophosphate. Therefore, the production of AMP in reactions assembled with BiP, ATP, and combinations of FICD enzymes was used to evaluate the relative contribution of AMPylation and de-AMPylation to the apparent inability of wildtype FICD to promote a pool of AMPylated BiP (Fig. 1 & 2c). No AMP was observed in reactions with the de-AMPylation defective FICD^{E234G}, consistent with stability of BiP$^{T518-AMP}$ (Fig. 5a, blue trace), however, substantial amounts of AMP were produced over time when wildtype FICD was included alongside the hyperactive mutant FICD^{E234G} (Fig. 5a, red trace and Fig. 5b). Importantly, AMP was not produced in reactions with wildtype FICD alone (Fig. 5a, black trace). These observations suggest that in the absence of other yet-to-be-identified cellular components the wildtype enzyme is locked in an AMPylation incompetent state, as suggested previously [16,17], although it cannot be excluded that the in vitro assay conditions used here selectively interfere with the AMPylation activity of the wildtype enzyme. However, the wildtype enzyme freely de-AMPylates BiP and a single FICD^{E234G} mutation flips the activity of FICD from a constitutive de-AMPylase to a pure AMPylase.

Cellular effects of FICD overexpression

To explore the role of FICD as a BiP de-AMPylating enzyme in vivo, the effect of oveexpression of the wildtype enzyme on the level of AMPylated BiP was analyzed in wildtype CHO-K1 cells. Exposure to cycloheximide rapidly led to the emergence of a strong signal of AMPylated BiP, detected by its characteristic mobility on native-PAGE gels ('B' form) [12]. This signal was progressively attenuated by overexpression of wildtype FICD (Fig. 6a), consistent with de-AMPylation of endogenous BiP by overexpressed FICD.

BiP potently represses UPR signaling [25,26], whereas inactivation of BiP, by enforced AMPylation, induces the UPR [12]. A role for endogenous FICD in BiP de-AMPylation predicts more UPR activity in *FICD$^{-/-}$* cells targeted with de-AMPylation defective, AMPylation competent FICD derivatives than in similarly-targeted wildtype cells. To test this prediction, the intensity of the UPR was compared between isogenic wildtype and *FICD$^{-/-}$* UPR reporter-bearing CHO-K1 cells transfected with plasmids encoding FICD derivatives. Expression of the catalytically-inactive FICD$^{E234G-H363A}$, at similar levels to wildtype FICD, had no effect on UPR signaling, suggesting an insignificant increase in the unfolded protein load by expression of either FICD. Moreover, de-AMPylation defective, AMPylation competent FICD derivatives with mutations at E234, reproducibly induced more UPR signaling in the *FICD$^{-/-}$* cells (Fig. 6b & Supplementary Fig. 3). Conversely, co-

expression of the de-AMPylation competent wildtype FICD attenuated both accumulation of AMPylated endogenous BiP and UPR signaling induced by the hyperactive FICD[E234G] (Fig. 6c & Supplementary Fig. 4). Treatment with the ER stress-inducing compounds tunicamycin or thapsigargin, or transfection of effector plasmids expressing the Cas9 nuclease and single guide RNAs that target the BiP gene promoted similar levels of UPR signaling in wildtype and *FICD*^{-/-} cells (Supplementary Fig. 5), attesting to the selective sensitization by the *FICD*^{-/-} genotype towards effectors that inactivate BiP by AMPylation.

BiP inactivation has a large fitness cost [12,24]. In keeping with a role for endogenous FICD in reversing BiP inactivation by AMPylation, wildtype CHO-K1 cells tolerated stable expression of a retrovirus encoding the de-AMPylation defective, AMPylation-competent FICD[E234G] better than *FICD*^{-/-} mutant cells (Fig. 6d). Together, these observations point to a role for endogenous FICD in reversing BiP AMPylation and restoring chaperone activity in cells.

Discussion

FICD is both necessary and sufficient for BiP inactivation by AMPylation. The same enzyme is implicated here in removing this modification and in BiP reactivation. The side chain of a single residue, E234 determines which of the two opposing activities FICD will manifest in vitro. Under the conditions of our assay, E234 of wildtype FICD blocks all BiP AMPylation and renders the enzyme a pure de-AMPylase of BiP. Substitutions at E234, abolish the BiP-directed de-AMPylase activity of FICD and unmask, to varying degrees, its BiP AMPylating activity.

FICD's E234 lies at the tip of a regulatory helix conserved in other FIC enzymes [21–23] (Fig. 7). Engagement of the E234 side-chain in the active site sterically and electronically, delocalizes the terminal phosphates of the bound ATP to repress AMPylation [16,17], explaining why, in absence of other factors, wildtype FICD is inactive as an AMPylase. However, the E234 side-chain is flexible, and while engaged in the active site can either form a salt bridge with FICD's R374 or retain its charged group free to engage in alternative reactions (PDB 4uO4 and 4uOU) such as BiP de-AMPylation.

In vitro, the two forms of FICD, wildtype and E234G, represent the extremes of two opposing enzymatic activities. It is likely that other components, present in the ER, specify which of the two activities will prevail at any time, thus sparing the cell fruitless cycles of ATP-consuming, BiP AMPylation and de-AMPylation. It is tempting to speculate that a mechanism exists for coupling the disposition of the E234-containing helix to the burden of unfolded protein in the ER, such that when this burden is high the E234 side-chain is engaged in the active site to block AMPylation and favor de-AMPylation. This appears to be the default conformation of pure FICD, explaining its inability to AMPylate BiP and its constitutive BiP de-AMPylating activity in vitro. When the burden of unfolded proteins is low, a conformational switch in FICD disengages the E234 side chain to promote AMPylation. This proposed short-term mechanism for regulating FICD's intrinsic enzymatic activity functions alongside circuits known to regulate the level of the enzyme, notably the UPR [10–12].

The mechanism behind this in vivo switch remains to be worked out, nonetheless the dominance of de-AMPylation over AMPylation when the wildtype enzyme is overexpressed, suggests that in the ER too the default state of E234 is to engage the active site and that an active mechanism, triggered in vivo when the burden of unfolded proteins is low, pries E234 from the active site converting wildtype FICD to an AMPylase. The machinery for switching FICD from de-AMPylation to AMPylation is absent from the in vitro assays conducted here but the consequences of its action are mimicked by the E234G mutation, which locks FICD in a constitutively AMPylating mode (Fig. 7).

The FIC domain is highly flexible in terms of substrate utilization. The bacterial FIC protein DOC has been observed both to phosphorylate threonine 382 of bacterial EF-Tu and to dephosphorylate the same residue. Analysis of the reaction products indicates that DOC mediated de-phosphorylation is achieved by thermodynamically-unfavored reversal of the phosphorylation reaction, re-generating a nucleotide tri-phosphate 27. By contrast the reaction products of FICD-mediated BiP de-AMPylation (unmodified BiP and free AMP) argue against simple mass action-driven enzymatic micro-reversibility and suggest instead that the active site of FICD is exploited for two interdependent, physiologically-antagonistic, chemically-distinct reactions.

AMPylation by FIC-domain enzymes employs a conserved HPFx(D/E)GN(G/K)R catalytic loop to position the attacking nucleophile in close proximity to the α-phosphate of the bound ATP substrate 28–30. A co-crystal structure of the bacterial enzyme, IbpA, and its AMPylated target, Cdc42, indicates that the same pocket in the FIC active site can accommodate adenosine-phosphate when it is part of the ATP substrate and as part of the AMPylated Cdc42 product 28. Both AMPylation and de-AMPylation by FICD require the conserved H363. Thus, a shared active site residue contributes to two antagonistic reactions initiated by different attacking nucleophiles.

In AMPylation, FICD mediates a concerted deprotonation and attack of the T518 hydroxyl of BiP on the α-phosphate of the bound ATP substrate 17,28. In de-AMPylation the hydroxyl of a water molecule, likely activated by E234, may attack the phosphodiester bond of the bound AMP. It is tempting to speculate that the essential role of FICD's H363 in both reactions reflects deprotonation of the attacking nucleophile in the AMPylation reaction and protonation of the BiP T518 leaving group in the de-AMPylation reaction.

Our analysis has been restricted to a single FIC enzyme, FICD, and to a single substrate, BiP. The role, if any, of FIC enzymes, and FICD in particular, in de-modifying other substrates, remains to be explored. Nor is it known if all the functional consequences of FICD inactivation can be understood in the context of the enzymes' role in regulating BiP activity. But in that context, the findings presented here are consistent with a model whereby BiP AMPylation evolved as an additional cellular buffer to fluctuations in unfolded ER proteins by acquisition of a single dual-functioning enzyme whose activity is switched in vivo by positioning a conserved regulatory residue. Because BiP AMPylation responds directly to changes in unfolded protein load, without need for gene expression or protein synthesis 11, the machinery for executing this switch may tell us something about the most proximal steps in protein folding homeostasis in the ER.

Methods

Cell lines

All cells were grown on tissue culture dishes or multi-well plates (Corning) at 37°C and 5% CO_2. CHO-K1 cells (ATCC CCL-61) were phenotypically validated as proline auxotrophs and their *Cricitulus griseus* origin was confirmed by genomic sequencing. The cells were cultured in Nutrient mixture F-12 Ham (Sigma) supplemented with 10% (v/v) serum (FetalClone II; HyClone), 1 x Penicillin-Streptomycin (Sigma) and 2 mM L-glutamine (Sigma). The CHO-K1 *FICD*^{-/-} cell lines used in this study were described previously [12].

HEK293T cells (ATCC CRL-3216) were cultured in Dulbecco's Modified Eagle's Medium (Sigma) supplemented as described above.

Cell lines were subjected to random testing for mycoplasma contamination using the MycoAlert Mycoplasma Detection Kit (Lonza). Experiments were performed at cell densities of 60-90% confluence. Cells were treated with drugs at the following final concentrations: 100 μg/ml cycloheximide (Sigma), 2.5 μg/ml tunicamycin (Melford), 0.5 μM thapsigargin (Calbiochem), and 6-8 μg/ml puromycin (Calbiochem). All drugs were first diluted in fresh, pre-warmed medium and then applied to the cells by medium exchange.

Detailed information on flow cytometry analysis procedures, and production of VSV-G retroviral virus in HEK293T cells and infection of CHO-K1 cells can be found in Supplementary Note.

Mammalian cell lysates

Cell lysis was performed as described in 6 with modifications. In brief, mammalian cells were cultured on 10 cm dishes and treated as indicated and/or transfected using Lipofectamine LTX with 5 μg plasmid DNA unless indicated otherwise, and allowed to grow for 24 hours. Before lysis the dishes were placed on ice, washed with ice-cold PBS, and cells were detached in PBS containing 1 mM EDTA using a cell scraper. The cells were sedimented for 5 minutes at 370 *g* at 4°C and lysed in HG lysis buffer [20 mM HEPES-KOH pH 7.4, 150 mM NaCl, 2 mM $MgCl_2$, 10 mM D-glucose, 10% (v/v) glycerol, 1% (v/v) Triton X-100] containing protease inhibitors (2 mM PMSF, 4 μg/ml pepstatin, 4 μg/ml leupeptin, 8 μg/ml aprotinin) with 100 U/ml hexokinase (from *Saccharomyces cerevisiae* Type F-300; Sigma) for 10 minutes on ice. The lysates were cleared for 10 minutes at 21,000 *g* at 4°C. BIO-RAD protein assay reagent (BioRad) was used to determine the protein concentrations of lysates followed by normalization. For analysis by SDS-PAGE, SDS sample buffer was added to the lysates and proteins were denatured by heating for 10 minutes at 70°C before separation on 12.5% SDS polyacrylamide gels. To detect endogenous BiP by native-PAGE the lysate samples were loaded immediately on native gels (see below).

Plasmid construction

Supplementary Table 1 lists the plasmids used in this study. Standard PCR and molecular cloning methods were used to generate DNA constructs and point mutations were introduced by PCR-based site-directed mutagenesis.

Protein purification

N-terminally hexahistidine- (His6-) tagged wildtype and mutant Chinese hamster BiP proteins were expressed in M15 *E. coli* cells (Qiagen). The bacterial cultures were grown at 37°C to an optical density ($OD_{600\ nm}$) of 0.8 in LB medium supplemented with 50 μg/ml kanamycin and 100 μg/ml ampicillin and expression of recombinant protein was induced by the addition of 1 mM isopropylthio β-D-1-galactopyranoside (IPTG). The cells were further incubated at 37°C for 6 hours, harvested by centrifugation, and lysed with a high-pressure homogenizer (EmulsiFlex-C3, Avestin) in buffer A [50 mM Tris-HCl pH 7.5, 500 mM NaCl, 1 mM MgCl$_2$, 0.2% (v/v) Triton X-100, 10% (v/v) glycerol, 20 mM imidazole] containing protease inhibitors [2 mM phenylmethylsulphonyl fluoride (PMSF), 4 μg/ml pepstatin, 4 μg/ml leupeptin, 8 μg/ml aprotinin] and 0.1 mg/ml DNaseI. The obtained lysates were cleared by centrifugation for 30 minutes at 25,000 *g* and incubated with 1 ml Ni-NTA agarose (Qiagen) per 1 l of expression culture for 2 hours at 4°C. The matrix was transferred to a column and washed five times with 20 bed volumes of buffer A containing 5 mM β-mercaptoethanol and supplemented sequentially with (i) 30 mM imidazole, (ii) 1% (v/v) Triton X-100, (iii) 1 M NaCl, (iv) 5 mM Mg^{2+}-ATP, or (v) 0.5 M Tris-HCl pH 7.5. Bound BiP proteins were eluted in buffer B [50 mM HEPES-KOH pH 7.5, 300 mM NaCl, 10% (v/v) glycerol, 5 mM β-mercaptoethanol, 250 mM imidazole] and dialyzed against HKM buffer [50 mM HEPES-KOH pH 7.4, 150 mM KCl, 10 mM MgCl$_2$]. The proteins were concentrated using centrifugal filters (Amicon Ultra, 30 kDa MWCO; Merck Millipore), snap-frozen in liquid nitrogen, and stored at -80°C.

Bacterial expression and purification of N-terminally GST-tagged wildtype and mutant FICD proteins was performed according to 12 with modifications. The FICD-encoding DNA constructs were transformed into C3013 BL21 T7 Express *lysY/Iq E. coli* cells (New England BioLabs) and cultures of single clones were grown at 37°C in LB medium containing 100 μg/ml ampicillin. At an $OD_{600\ nm}$ of 0.8 the cultures were shifted to 20°C and expression was induced with 0.5 mM IPTG. After incubation for 16 hours the cells were harvested and lysed as described above in lysis buffer [50 mM Tris-HCl pH 7.5, 500 mM NaCl, 1 mM MgCl$_2$, 2 mM dithiothreitol (DTT), 0.2% (v/v) Triton X-100, 10% (v/v) glycerol] containing protease inhibitors and DNaseI. The lysates were cleared by centrifugation for 30 minutes at 25,000 *g* and incubated with 0.7 ml Glutathione Sepharose 4B (GE Healthcare) per 1 l of expression culture for 2 hours at 4°C. The beads were washed with 20 ml wash buffer C [50 mM Tris-HCl pH 7.5, 500 mM NaCl, 1 mM DTT, 0.2% (v/v) Triton X-100, 10% (v/v) glycerol] containing protease inhibitors, 20 ml wash buffer D [50 mM Tris-HCl pH 7.5, 300 mM NaCl, 10 mM MgCl$_2$, 1 mM DTT, 0.1% (v/v) Triton X-100, 10% (v/v) glycerol] containing protease inhibitors and 20 ml wash buffer D sequentially supplemented with (i) 1% (v/v) Triton X-100, (ii) 1 M NaCl, (iii) 3 mM ATP, or (iv) 0.5 M Tris-HCl pH 7.5. Bound proteins were eluted in elution buffer [50 mM HEPES-KOH pH 7.4, 100 mM KCl, 4 mM MgCl$_2$, 1 mM CaCl$_2$, 0.1% (v/v) Triton X-100, 10% (v/v)

glycerol, 40 mM reduced glutathione] and concentrated protein solutions were frozen in liquid nitrogen and stored at -80°C. For preparation of wildtype FICD without the GST-tag the protein was eluted from glutathione-Sepharose in elution buffer without Triton X-100 and with 1.5 mM DTT. TEV protease was added in a 100:1 (protein-to-TEV) molar ratio and after incubation for 16 hours at 4°C the proteins were passed over a size-exclusion chromatography column (Superdex 200 10/300 GL; GE Healthcare) in HKMG buffer [50 mM HEPES-KOH pH 7.4, 150 mM KCl, 10 mM MgCl$_2$, 10% glycerol]. The FICD protein-containing fractions were pooled, concentrated, and frozen in aliquots.

Purification of in vitro AMPylated BiP proteins

AMPylated BiP proteins were prepared as described previously [12], with modifications. In brief, 20 mg of purified wildtype BiP or substrate-binding deficient BiP^{V461F} mutant protein [31] was in vitro AMPylated for 4 hours at 30°C with 0.25 mg bacterially expressed FICD^{E234G} in presence of 3 mM ATP in buffer E [25 mM HEPES-KOH pH 7.4, 100 mM KCl, 10 mM MgCl$_2$, 1 mM CaCl$_2$, 0.1% (v/v) Triton X-100]. Afterwards, BiP proteins were bound to 400 μl Ni-NTA agarose affinity matrix for 30 minutes at 25°C, washed with buffer E, and eluted in buffer E containing 350 mM imidazole for 45 minutes at 25°C. The eluate was concentrated and passed over a Centri•Pure P25 desalting column (emp BIOTECH) equilibrated in HKMG buffer. The protein-containing fractions were pooled, concentrated, frozen in liquid nitrogen, and stored at -80°C. BiP was quantitatively AMPylated as judged by the conversion of BiP oligomers into the modified monomeric 'B' form on a native-PAGE gel. The modified BiP proteins were used for in vitro de-AMPylation assays and mass spectrometry analysis (see below). Unmodified BiP prepared from a parallel mock AMPylation reaction without enzyme served as a control.

In vitro AMPylation and de-AMPylation assays

Unless stated otherwise in vitro AMPylation and de-AMPylation reactions were performed in AMPylation buffer [25 mM HEPES-KOH pH 7.4, 100 mM KCl, 4 mM MgCl$_2$, 1 mM CaCl$_2$, 0.1% (v/v) Triton X-100].

Radioactive in vitro AMPylation (Fig. 2c) reactions were set up in a final volume of 37.5 μl containing 1 μM of ATP hydrolysis-deficient mutant BiP protein (BiP^{T229A}) [32], 0.1 μM wildtype or mutant FICD proteins, 40 μM ATP, and 0.023 MBq α-^{32}P-ATP (EasyTide; Perkin Elmer). The reactions were started by addition of the nucleotides and incubated at 25°C. After 3 and 10 minutes of incubation 15 μl were removed from each reaction, respectively, supplemented with 5 μl SDS sample buffer, heated for 5 minutes at 75°C and loaded on a SDS-PAGE gel. Gels were stained with Coomassie and the radioactive signals were detected with a Typhoon Trio imager (GE Healthcare) upon overnight exposure of the dried gels to a storage phosphor screen.

For radioactive de-AMPylation experiments (Fig. 2a) BiP was first AMPylated in vitro with α-^{32}P-ATP and then re-purified. Therefore, 6 μg of purified BiP was pre-incubated with 15 μM ATP in a final volume of 20 μl in AMPylation buffer for one minute at 25°C before 1.85 MBq α-^{32}P-ATP and 2 μg FICD^{E234G} was added. The mixture was incubated for 10 minutes at 25°C and another 12 μg of BiP was added. After further incubation for 50 minutes the

reaction was diluted with 200 μl of high-salt AMPylation buffer [25 mM HEPES-KOH pH 7.4, 500 mM KCl, 4 mM MgCl$_2$, 1 mM CaCl$_2$, 0.1% (v/v) Triton X-100] and 1 mM ATP was added. BiP was then bound to 20 μl Ni-NTA agarose beads for 30 minutes at 20°C. The beads were washed with 500 μl high-salt AMPylation buffer containing 1 mM ATP and three times with high-salt AMPylation buffer. Bound proteins were eluted in 100 μl AMPylation buffer containing 400 mM imidazole (pH 7.4) for 30 minutes at 20°C. The eluate was split in two fractions of 50 μl and each fraction was passed through a Sephadex G-50 MicroSpin column (illustra AutoSeq G-50; GE Healthcare) equilibrated with AMPylation buffer, and the recovered proteins were frozen in aliquots until the de-AMPylation experiment. The de-AMPylation reactions were carried out at 23°C in a final volume of 15 μl in AMPylation buffer containing 1.3 μg non-radioactive AMPylated wildtype BiP supplemented with trace amounts of radiolabelled AMPylated BiP ($\approx$ 0.1 μg). The reactions were started at different time points by addition of 0.13 μg wildtype or mutant FICD. At the end of the experiment 5 μl SDS sample buffer were added to each reaction, proteins were denatured for 5 minutes at 75°C, and 15 μl of each sample were applied to SDS-PAGE. After separation, the proteins were stained with Coomassie to confirm equal loading and radioactive signals were detected by autoradiography as described above.

The non-radioactive de-AMPylation reactions shown in Fig. 3d contained 1 μg/μl purified AMPylated wildtype BiP, 0.1 μg/μl wildtype or mutant FICD, and were incubated for 90 minutes at 30°C in a final volume of 25 μl in presence of 3 mM ATP. Afterwards, each reaction was divided in two samples, one of which was treated for 10 minutes with 0.06 μg/μl SubA protease at 25°C, whereas the other remained untreated. The samples were then supplemented with native sample buffer and analysed immediately by native-PAGE and Coomassie staining (see below). The de-AMPylation reactions shown in Fig. 3e were performed in HKM buffer and contained 1 μg/μl purified AMPylated or unmodified wildtype BiP and were incubated without or with 0.05 μg/μl wildtype FICD for 30 minutes at 30°C in absence of ATP (to allow re-formation of BiP oligomers) before analysis by native-PAGE.

The reactions shown in Fig. 2b contained 3 μg/μl protein from lysates of untreated wildtype CHO-K1 cells or cells treated for 3 hours with CHX, and 0.15 μg/μl purified wildtype or mutant FICD (see above). The reactions were started by addition of purified FICD and incubated at 30°C. After 15 minutes, the reactions were diluted 1:10 in IEF lysis buffer and analysed by IEF (see below).

Detailed information on Fluorescence polarization assay procedures can be found in Supplementary Note.

Mass spectrometry

For mass spectrometry analysis purified in vitro AMPylated or unmodified wildtype BiP (Chinese hamster) at 16 μM was incubated with 0.8 μM wildtype FICD or catalytically inactive mutant FICD[H363A] for 3 hours at 30°C. Afterwards, the proteins were denatured with SDS sample buffer, heated for 5 minutes at 75°C, and separated by SDS-PAGE. The gels were stained with Coomassie, destained, and the bands at 75 kDa corresponding to BiP protein were excised. The proteins were then reduced, alkylated, and digested "in-gel" with

Arg-C proteinase. The obtained peptides were analyzed by LC-MS using a Q Exactive mass spectrometer (Thermo Fischer) coupled to a RSLC 3000 UHPLC. The data were processed with Proteome Discoverer 1.4 using Sequest to search a Uniprot E. coli database (downloaded 29/04/15, 4377 entries) with the sequence of Chinese hamster (*Cricetulus griseus*) BiP added. Oxidation (M) and AMPylation (S/T) were set as variable modifications and carbamidomethylation (C) as a fixed modification. FDR calculations were performed by Percolator and peptides were filtered to 1%.

Ion pair chromatography (IPC)

To detect the leaving group of the FICD-mediated de-AMPylation reaction, reversed-phase IPC was performed (Fig. 3c). Purified in vitro AMPylated or unmodified BiP proteins at 65 μM were exposed to wildtype FICD or mutant FICD[H363A] proteins at 6.5 μM in HKM buffer in a final volume of 30 μl for 2 hours at 30°C. At the end of the incubation time the reactions were stopped by addition of 10 μl of 4 M perchloric acid (PCA). As a negative control AMPylated BiP was incubated in parallel for 2 hours without enzyme and FICD was added directly before mixing with PCA. After incubation for 5 minutes on ice the samples were centrifuged at 21,000 g for 2 minutes at 4°C and 32 μl of the supernatants were mixed with 20 μl of 2 M potassium hydroxide (KOH). The pH of the samples was neutralized, the precipitates were sedimented by centrifugation for 15 minutes at 21,000 g at 4°C, and the cleared supernatant were equilibrated to room temperature before analysis by IPC. For that, 20 μl of each sample were injected onto a Poroshell 120 EC-C18 HPLC column (3 x 150 mm, 2.7 μm; Agilent Technologies) connected to a UHPLC Guard column (Agilent Technologies). Buffers A [H_2O + 10 mM tetrabutylammonium hydroxide (TBAH) + 10 mM potassium dihydrogen phosphate (KH_2PO_4)] and B [methanol (CH_3OH) + 10 mM TBAH] were used as a mobile phase. The runs were performed at a constant flow rate of 0.4 ml/min at room temperature using the following gradient: 5% to 50% B in 25 minutes, hold for 2 minutes at 50% B, ramp to 95% B in 0.1 minute, hold for 7 minutes, 95% to 5% B in 1 minute, hold for 5 minutes at 5% B (re-equilibration to basal). Nucleotide absorbance traces at 254 nm ($A_{254\ nm}$) were recorded and plotted against elution time. A nucleotide standard was applied in each experiment to determine the retention times of ATP, ADP and AMP.

Coupled AMPylation/de-AMPylation reactions (Fig. 3d and Supplementary Fig. 2) contained 20 μM ATP hydrolysis-deficient BiP[T229A], 2 μM wildtype FICD, 2 μM FICD[E234G], and 2 mM ATP in HKM buffer as indicated and were incubated for 3 hours at 30°C before deproteination and HPLC analysis as described above.

Native polyacrylamide gel electrophoresis (native-PAGE)

Non-denaturing native-PAGE was performed as described 6. Briefly, Tris-glycine polyacrylamide gels (4.5% stacking gel and a 7.5% separation gel) were used to separate purified proteins or proteins from mammalian cell lysates to detect BiP oligomers. The separation was performed in running buffer (25 mM Tris, 192 mM glycine, pH ~8.8) at 120 V for 2 hours. Afterwards, the proteins were visualized by staining with InstantBlue Coomassie solution (expedeon) or transferred to a polyvinylidene difluoride (PVDF) membrane in blotting buffer (48 mM Tris, 39 mM glycine; pH ~9.2) supplemented with 0.04 (w/v) SDS for 16 hours at 30 V for immunodetection. The membrane was washed for 20

minutes in blotting buffer (without SDS) supplemented with 20% (v/v) methanol before blocking. Seven μg of purified BiP protein was loaded per lane to detect purified BiP proteins by Coomassie staining and volumes of lysates corresponding to 30 μg of total protein were loaded per lane to detect endogenous BiP from CHO-K1 cell lysates by immunoblotting.

Immunoblot analysis

After separation by SDS-PAGE or native-PAGE (see above) the proteins were transferred onto PVDF membranes. The membranes were blocked with 5% (w/v) dried skimmed milk in TBS (25 mM Tris-HCl pH 7.5, 150 mM NaCl) and incubated with primary antibodies followed by IRDye fluorescently labeled secondary antibodies (LiCor). The membranes were scanned with an Odyssey near-infrared imager (LiCor). Primary antibodies and antisera against hamster BiP [chicken anti-BiP; 33], eIF2α [mouse anti-eIF2α; 34], and FICD [chicken anti-FICD 12] were used.

Isoelectric focusing (IEF)

Analysis of lysates from mammalian cells by IEF was performed as described previously 12. Cells were grown in 10 cm dishes to approximately 90% confluence and treated with cycloheximide for 3 hours. Afterwards, the cells were washed with ice-cold TBS, resuspended in 1 ml TBS, sedimented by centrifugation, and lysed in 30 x its packed cell pellet volume of IEF lysis buffer [8.8 M urea, 5% (w/v) CHAPS, 1 μM sodium pyrophosphate, 2 mM imidodiphosphate, 50 mM DTT, 2% (v/v) Pharmalyte] at room temperature for 5 minutes. The lysates were centrifuged at 21,000 g for 10 minutes at room temperature and the resulting supernatants were centrifuged again for 60 minutes. The cleared lysates were passed over a Sephadex G-50 MicroSpin columns equilibrated with IEF sample buffer [8 M urea, 5% (w/v) CHAPS, 50 mM DTT, 2% (v/v) Pharmalyte (pH 4.5-5.4; GE Healthcare)], and 15 μl loaded on a 3.75% polyacrylamide gel containing 8.8 M urea, 1.25% (w/v) CHAPS, and 5% (v/v) Pharmalyte. The wells were overlaid with 0.5 M urea and 2% (v/v) Pharmalyte solution before the run. The anode buffer was 10 mM glutamic acid and the cathode buffer was 50 mM histidine. The run was performed as follows: 100 V for 10 minutes, 250 V for 1 hour, 300 V for 1 hour, 500 V for 30 minutes. The proteins were then transferred to a nitrocellulose membrane for 3 hours at 300 mA in blotting buffer [25 mM Tris-HCl pH 9.2, 190 mM glycine, 0.01% (w/v) SDS, 10% (v/v) methanol] and BiP was detected as described above.

Data availability

The authors declare that the data supporting the findings of this study are available within the paper and its supplementary information files. Source data for Fig. 6 and supplementary Fig. 5 are provided with the paper online.

Supplementary Material

Refer to Web version on PubMed Central for supplementary material.

Acknowledgements

References

1. Balch WE, Morimoto RI, Dillin A, Kelly JW. Adapting proteostasis for disease intervention. Science. 2008; 319:916–919. doi:319/5865/916 [pii]. DOI: 10.1126/science.1141448 [PubMed: 18276881]

2. Wang M, Kaufman RJ. Protein misfolding in the endoplasmic reticulum as a conduit to human disease. Nature. 2016; 529:326–335. DOI: 10.1038/nature17041 [PubMed: 26791723]

3. Walter P, Ron D. The unfolded protein response: from stress pathway to homeostatic regulation. Science. 2011; 334:1081–1086. DOI: 10.1126/science.1209038 [PubMed: 22116877]

4. Freiden PJ, Gaut JR, Hendershot LM. Interconversion of three differentially modified and assembled forms of BiP. EMBO J. 1992; 11:63–70. [PubMed: 1740116]

5. Chevalier M, King L, Wang C, Gething MJ, Elguindi E, Blond SY. Substrate binding induces depolymerization of the C-terminal peptide binding domain of murine GRP78/BiP. J Biol Chem. 1998; 273:26827–26835. [PubMed: 9756927]

6. Preissler S, Chambers JE, Crespillo-Casado A, Avezov E, Miranda E, Perez J, Hendershot LM, Harding HP, Ron D. Physiological modulation of BiP activity by *trans*-protomer engagement of the interdomain linker. Elife. 2015; 4:e08961.doi: 10.7554/eLife.08961 [PubMed: 26473973]

7. Laitusis AL, Brostrom MA, Brostrom CO. The dynamic role of GRP78/BiP in the coordination of mRNA translation with protein processing. J Biol Chem. 1999; 274:486–493. [PubMed: 9867869]

8. Chambers JE, Petrova K, Tomba G, Vendruscolo M, Ron D. ADP ribosylation adapts an ER chaperone response to short-term fluctuations in unfolded protein load. J Cell Biol. 2012; 198:371–385. DOI: 10.1083/jcb.201202005 [PubMed: 22869598]

9. Carlsson L, Lazarides E. ADP-ribosylation of the Mr 83,000 stress-inducible and glucose-regulated protein in avian and mammalian cells: modulation by heat shock and glucose starvation. Proc Natl Acad Sci U S A. 1983; 80:4664–4668. [PubMed: 6576354]

10. Sanyal A, Chen AJ, Nakayasu ES, Lazar CS, Zbornik EA, Worby CA, Koller A, Mattoo S. A novel link between Fic (filamentation induced by cAMP)-mediated adenylylation/AMPylation and the unfolded protein response. J Biol Chem. 2015; 290:8482–8499. DOI: 10.1074/jbc.M114.618348 [PubMed: 25601083]

11. Ham H, Woolery AR, Tracy C, Stenesen D, Kramer H, Orth K. Unfolded protein response-regulated Drosophila Fic (dFic) protein reversibly AMPylates BiP chaperone during endoplasmic reticulum homeostasis. J Biol Chem. 2014; 289:36059–36069. DOI: 10.1074/jbc.M114.612515 [PubMed: 25395623]

12. Preissler S, Rato C, Chen R, Antrobus R, Ding S, Fearnley IM, Ron D. AMPylation matches BiP activity to client protein load in the endoplasmic reticulum. Elife. 2015; 4:e12621.doi: 10.7554/eLife.12621 [PubMed: 26673894]

13. Yarbrough ML, Li Y, Kinch LN, Grishin NV, Ball HL, Orth K. AMPylation of Rho GTPases by Vibrio VopS disrupts effector binding and downstream signaling. Science. 2009; 323:269–272. DOI: 10.1126/science.1166382 [PubMed: 19039103]

14. Worby CA, Mattoo S, Kruger RP, Corbeil LB, Koller A, Mendez JC, Zekarias B, Lazar C, Dixon JE. The fic domain: regulation of cell signaling by adenylylation. Mol Cell. 2009; 34:93–103. DOI: 10.1016/j.molcel.2009.03.008 [PubMed: 19362538]

15. Broncel M, Serwa RA, Bunney TD, Katan M, Tate EW. Global profiling of HYPE mediated AMPylation through a chemical proteomic approach. Mol Cell Proteomics. 2015; doi: 10.1074/mcp.O115.054429

16. Engel P, Goepfert A, Stanger FV, Harms A, Schmidt A, Schirmer T, Dehio C. Adenylylation control by intra- or intermolecular active-site obstruction in Fic proteins. Nature. 2012; 482:107–110. DOI: 10.1038/nature10729 [PubMed: 22266942]

17. Bunney TD, Cole AR, Broncel M, Esposito D, Tate EW, Katan M. Crystal structure of the human, FIC-domain containing protein HYPE and implications for its functions. Structure. 2014; 22:1831–1843. DOI: 10.1016/j.str.2014.10.007 [PubMed: 25435325]

18. Anderson WB, Stadtman ER. Glutamine synthetase deadenylation: a phosphorolytic reaction yielding ADP as nucleotide product. Biochem Biophys Res Commun. 1970; 41:704–709. [PubMed: 4920873]

19. Xu Y, Carr PD, Vasudevan SG, Ollis DL. Structure of the adenylylation domain of E. coli glutamine synthetase adenylyl transferase: evidence for gene duplication and evolution of a new active site. J Mol Biol. 2010; 396:773–784. DOI: 10.1016/j.jmb.2009.12.011 [PubMed: 20026075]

20. Neunuebel MR, Chen Y, Gaspar AH, Backlund PS Jr, Yergey A, Machner MP. De-AMPylation of the small GTPase Rab1 by the pathogen Legionella pneumophila. Science. 2011; 333:453–456. DOI: 10.1126/science.1207193 [PubMed: 21680813]

21. Garcia-Pino A, Zenkin N, Loris R. The many faces of Fic: structural and functional aspects of Fic enzymes. Trends Biochem Sci. 2014; 39:121–129. DOI: 10.1016/j.tibs.2014.01.001 [PubMed: 24507752]

22. Roy CR, Cherfils J. Structure and function of Fic proteins. Nat Rev Microbiol. 2015; 13:631–640. DOI: 10.1038/nrmicro3520 [PubMed: 26299785]

23. Harms A, Stanger FV, Dehio C. Biological Diversity and Molecular Plasticity of FIC Domain Proteins. Annu Rev Microbiol. 2016; doi: 10.1146/annurev-micro-102215-095245

24. Paton AW, Beddoe T, Thorpe CM, Whisstock JC, Wilce MC, Rossjohn J, Talbot UM, Paton JC. AB5 subtilase cytotoxin inactivates the endoplasmic reticulum chaperone BiP. Nature. 2006; 443:548–552. [PubMed: 17024087]

25. Bertolotti A, Zhang Y, Hendershot L, Harding H, Ron D. Dynamic interaction of BiP and the ER stress transducers in the unfolded protein response. Nat Cell Biol. 2000; 2:326–332. [PubMed: 10854322]

26. Pincus D, Chevalier MW, Aragon T, van Anken E, Vidal SE, El-Samad H, Walter P. BiP binding to the ER-stress sensor Ire1 tunes the homeostatic behavior of the unfolded protein response. PLoS Biol. 2010; 8:e1000415.doi: 10.1371/journal.pbio.1000415 [PubMed: 20625545]

27. Castro-Roa D, Garcia-Pino A, De Gieter S, van Nuland NA, Loris R, Zenkin N. The Fic protein Doc uses an inverted substrate to phosphorylate and inactivate EF-Tu. Nat Chem Biol. 2013; 9:811–817. DOI: 10.1038/nchembio.1364 [PubMed: 24141193]

28. Xiao J, Worby CA, Mattoo S, Sankaran B, Dixon JE. Structural basis of Fic-mediated adenylylation. Nat Struct Mol Biol. 2010; 17:1004–1010. DOI: 10.1038/nsmb.1867 [PubMed: 20622875]

29. Luong P, Kinch LN, Brautigam CA, Grishin NV, Tomchick DR, Orth K. Kinetic and structural insights into the mechanism of AMPylation by VopS Fic domain. J Biol Chem. 2010; 285:20155–20163. DOI: 10.1074/jbc.M110.114884 [PubMed: 20410310]

30. Khater S, Mohanty D. In silico identification of AMPylating enzymes and study of their divergent evolution. Sci Rep. 2015; 5:10804.doi: 10.1038/srep10804 [PubMed: 26039278]

31. Petrova K, Oyadomari S, Hendershot LM, Ron D. Regulated association of misfolded endoplasmic reticulum lumenal proteins with P58/DNAJc3. EMBO J. 2008; 27:2862–2872. doi:emboj2008199 [pii]. DOI: 10.1038/emboj.2008.199 [PubMed: 18923430]

32. Gaut JR, Hendershot LM. Mutations within the nucleotide binding site of immunoglobulin-binding protein inhibit ATPase activity and interfere with release of immunoglobulin heavy chain. J Biol Chem. 1993; 268:7248–7255. [PubMed: 8463260]

33. Avezov E, Cross BC, Kaminski Schierle GS, Winters M, Harding HP, Melo EP, Kaminski CF, Ron D. Lifetime imaging of a fluorescent protein sensor reveals surprising stability of ER thiol redox. J Cell Biol. 2013; 201:337–349. DOI: 10.1083/jcb.201211155 [PubMed: 23589496]

34. Scorsone KA, Panniers R, Rowlands AG, Henshaw EC. Phosphorylation of eukaryotic initiation factor 2 during physiological stresses which affect protein synthesis. J Biol Chem. 1987; 262:14538–14543. [PubMed: 3667588]
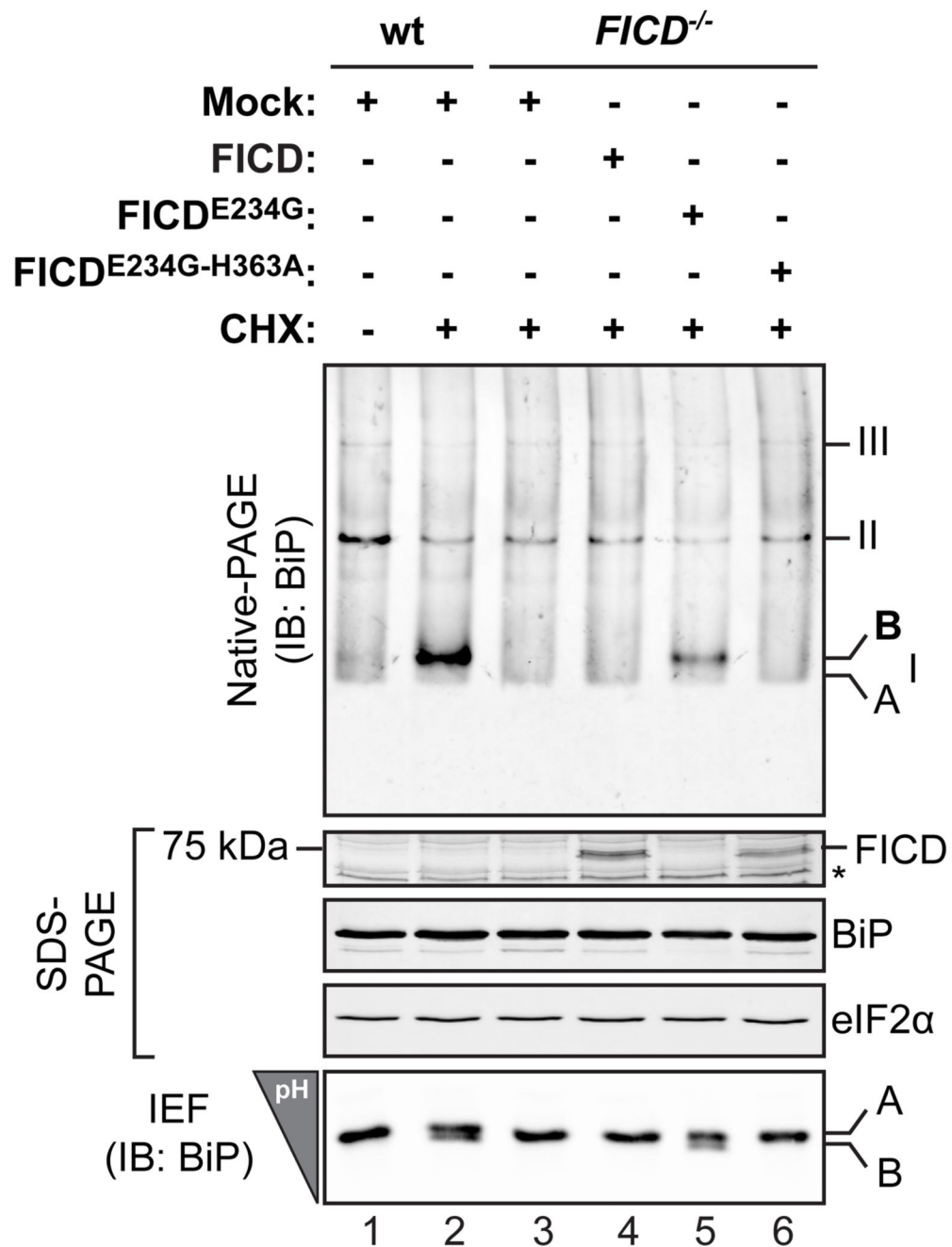
Figure 1. Introduction of wild type FICD into FICD deficient cells fails to restore BiP AMPylation

Immunoblot of endogenous BiP resolved by native gel electrophoresis from wildtype (wt) and FICD deficient (-/-) CHO-K1 cells transfected with plasmids encoding the indicated FICD derivatives and exposed to cycloheximide (CHX) to promote AMPylated BiP. The major species of BiP oligomers are numbered by order of descending mobility (I-III). The monomeric AMPylated 'B' form induced by CHX treatment and the 'A' form detectable in untreated cells are marked. Immunoblots of the same samples resolved by SDS-PAGE report on FICD, total BiP and total eIF2a (which also serves as a loading control) and the acidic

AMPylated 'B' form of BiP resolved by isoelectric focusing gel (IEF). The asterisk indicates a band of unknown identity. Data representative of four independent experiments are shown.

Uncropped blot images are shown in Supplementary Data Set 1.
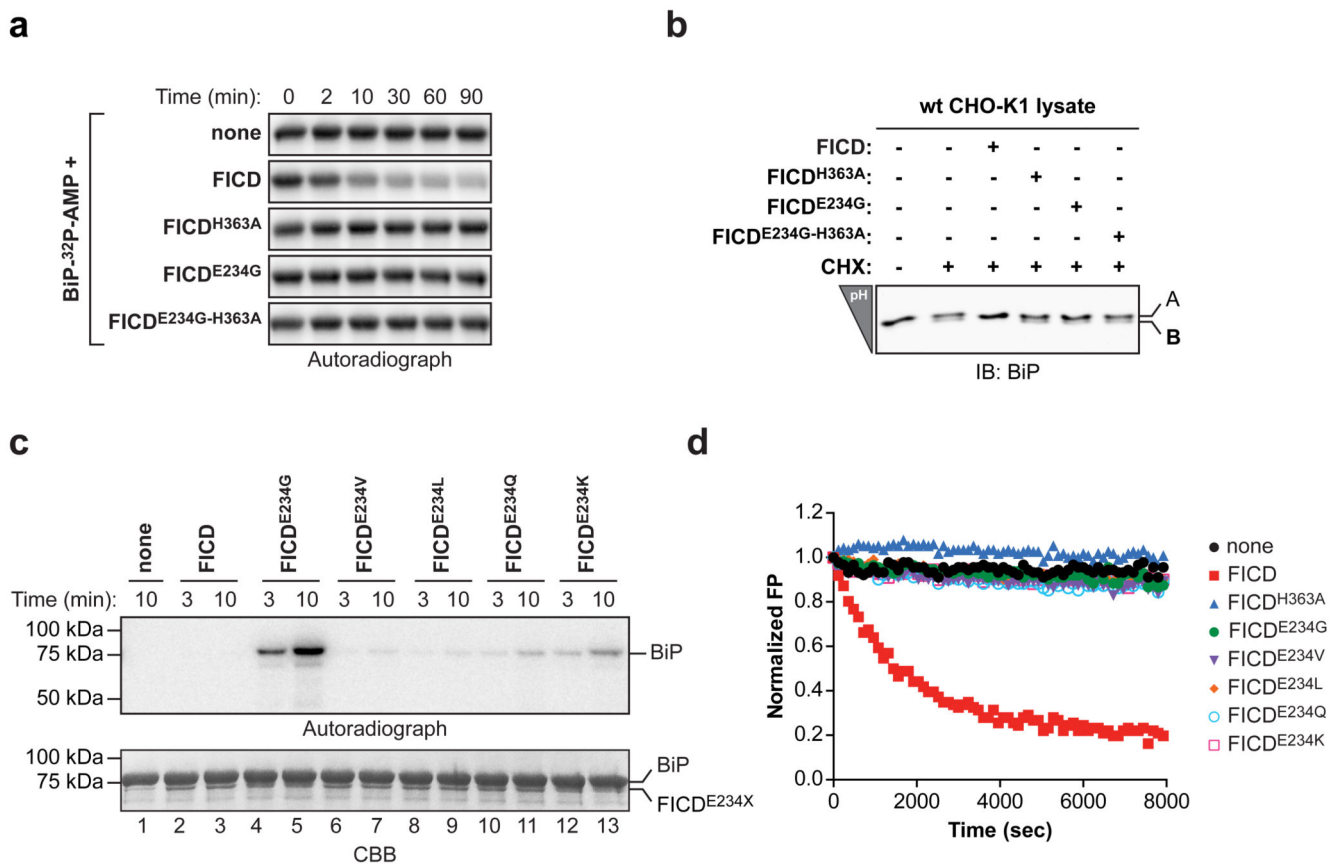
Figure 2. FICD de-AMPylates BiP in vitro

(**a**) Autoradiograph of an SDS-PAGE gel loaded with AMPylated BiP (BiP-^{32}P-AMP) that had been exposed to wildtype of mutant FICD for the indicated time Wildtype FICD-dependent de-AMPylation of BiP-^{32}P-AMP was observed in four independent experiments.

(**b**) IEF immunoblots of endogenous BiP from lysates of untreated or cycloheximide-treated (CHX) CHO-K1 cells that had been reacted in vitro with the indicated FICD enzymes.

(**c**) Autoradiograph and Coomassie stain (CBB) of an SDS-PAGE gel of BiP after exposure to wildtype or mutant versions of FICD in presence of α-^{32}P-ATP. A representative of three independent experiments is shown ($n = 3$).

(**d**) Time-dependent plot of fluorescence polarization (FP) of BiP AMPylated with FAM-labeled AMP (BiP$^{T518-AMP-FAM}$) following exposure to the indicated FICD proteins. The decrease in the FP signal reflects release of the fluorophore from BiP. A representative of five independent experiments is shown ($n = 5$).

Uncropped autoradiograph, gel and blot images are shown in Supplementary Data Set 1.
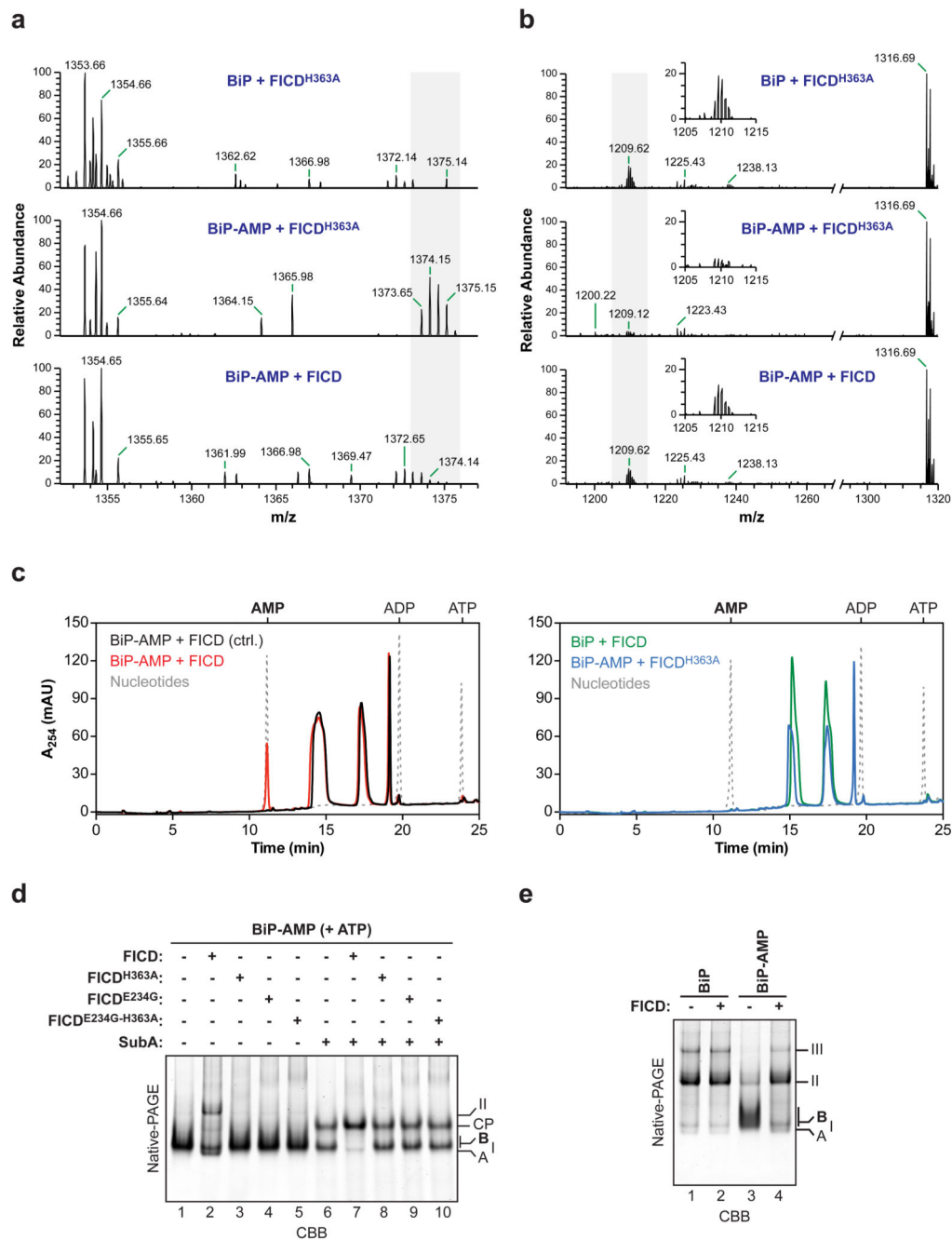
Figure 3. FICD-mediated de-AMPylation releases AMP and restores BiP to its pre-AMPylation state

(**a**) LC-MS spectra of peptides from an Arg-C digest of unmodified BiP protein (upper spectrum) or AMPylated BiP (BiP-AMP; lower two spectra) incubated with wildtype or FICD[H363A] mutant enzyme. The isotopic series of doubly charged ions derived from the AMPylated proteolytic BiP fragment (BiP[511-532]; 1374.15 m/z, z = 2) are highlighted in grey.

(**b**) As in "a" but showing the spectra of the unmodified BiP[511-532] peptides (1209.62 m/z, z = 2; isotopic ensemble highlighted in grey and magnified in the inset).

(**c**) Absorbance traces at 254 nm (A_{254} in milli absorbance units) of ion pair chromatograms of post-proteinaceous supernatants from samples of unmodified or in vitro AMPylated BiP after incubation with wildtype FICD or FICD[H363A]. The elution profile of known standards (ATP, ADP, and AMP) are indicated in grey dotted lines. In the control reaction (black trace on the left panel) the FICD enzyme was added to BiP-AMP followed immediately by deproteination. FICD-dependent appearance of an A_{254} absorbance peak at the AMP-specific elution time was observed in three independent experiments.

(**d**) CBB-stained native-PAGE gel of purified in vitro AMPylated BiP that had been subsequently exposed to the indicated FICD enzymes in presence of ATP, followed by further exposure to SubA protease where indicated. The migration of the non-AMPylated monomeric 'A' form (enriched in the presence of ATP), BiP dimers (II), the AMPylated 'B' form, and the nucleotide binding domain SubA cleavage product (CP) are noted. A representative result of three independent experiments is shown.

(**e**) As in "d", non-AMPylated and AMPylated BiP, resolved by native-PAGE but in the absence of ATP. A representative of three independent experiments is shown.

Uncropped gel images are shown in Supplementary Data Set 1.
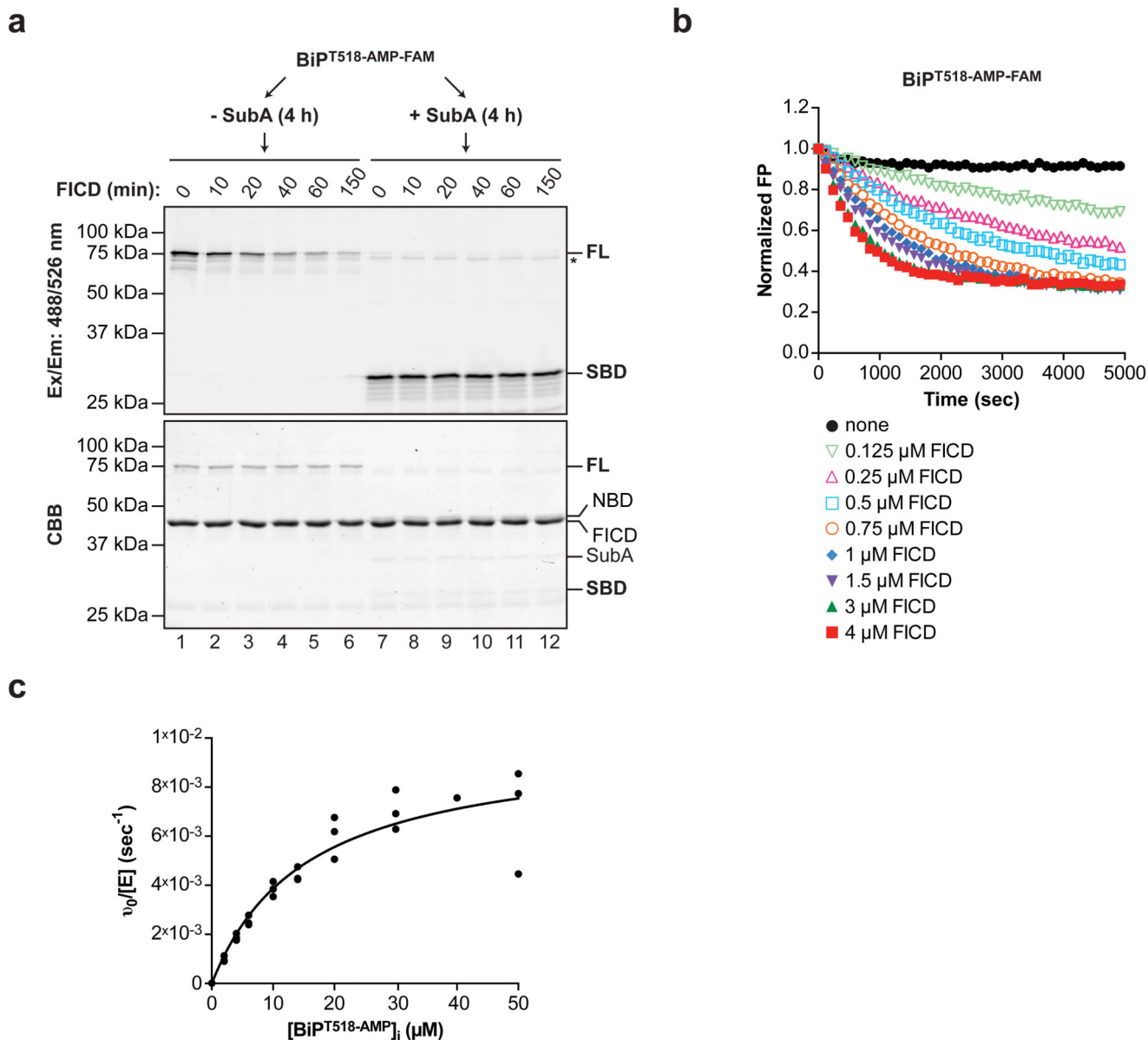
Figure 4. Enzymatic properties of the FICD de-AMPylase

(**a**) Fluorograph and Coomassie stain of intact or SubA cleaved BiP AMPylated with FAM-labeled AMP (BiP$^{T518-AMP-FAM}$) and exposed to wildtype FICD for the indicated time before SDS-PAGE. The location of full-length BiP (FL), the cleaved fluorescent substrate-binding (SBD), non-fluorescent nucleotide binding domain fragment (NBD), FICD and SubA are noted. The asterisk marks a high molecular weight fluorescent species distinct from full-length BiP$^{AMP-FAM}$ (FL) that is not a substrate for FICD-mediated de-AMPylation. A representative of two independent experiments is shown.

(**b**) Time-dependent plot of fluorescence polarization (FP) measurement of BiP$^{T518-AMP-FAM}$ (80 nM) exposed to increasing concentrations of wildtype FICD (0.125 to 4 μM) as indicated. A representative of four independent experiments is shown.

(**c**) Plot of the relation between initial substrate concentration $[BiP^{T518-AMP}]_i$ and the initial velocity of FICD-mediated de-AMPylation derived from change in FP of $BiP^{T518-AMP-FAM}$ (introduced as a tracer). Data points from three independent experiments and the non-linear fit curve are shown (K_M = 15.58 μM ± SD 3.27 μM and k_{cat} = 9.89 × 10^{-3} sec^{-1} ± SD 0.87 × 10^{-3} sec^{-1}).

Uncropped gel images are shown in Supplementary Data Set 1.
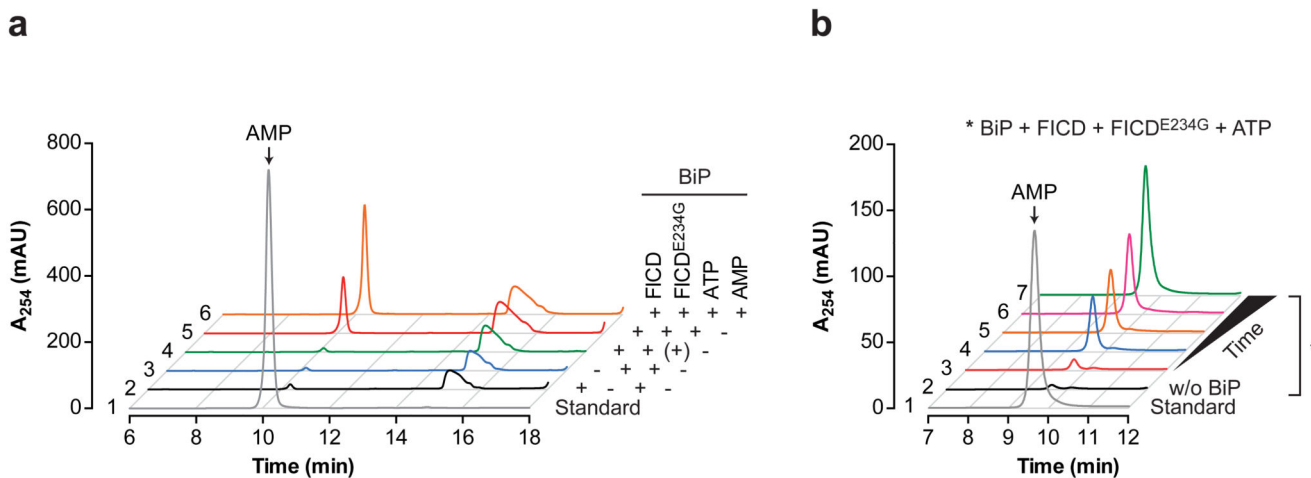
Figure 5. Engagement of E234 in the active site switches FICD from AMPylation to de-AMPylation

(**a**) Absorbance traces of the AMP-containing region of ion pair chromatograms of post-proteinaceous supernatants from samples derived from enzymatic reactions incorporating the indicated components. In the control reaction (trace 4, green) ATP was added followed immediately by deproteination. Trace 5 and 6 are of identical samples with the addition of AMP to trace 6 before chromatography (orange). Note that the appearance of an A_{254} absorbance peak at the AMP-specific elution time is restricted to the reaction containing both FICD[E234G] and wildtype FICD and was observed in four independent experiments.

(**b**) Absorbance traces (as above) of post-proteinaceous supernatants from a time course of the enzymatic reactions containing the indicated components. Trace 1 (grey line) is the elution profile of an AMP standard. A reaction without BiP (trace 2, black line) serves as a control.
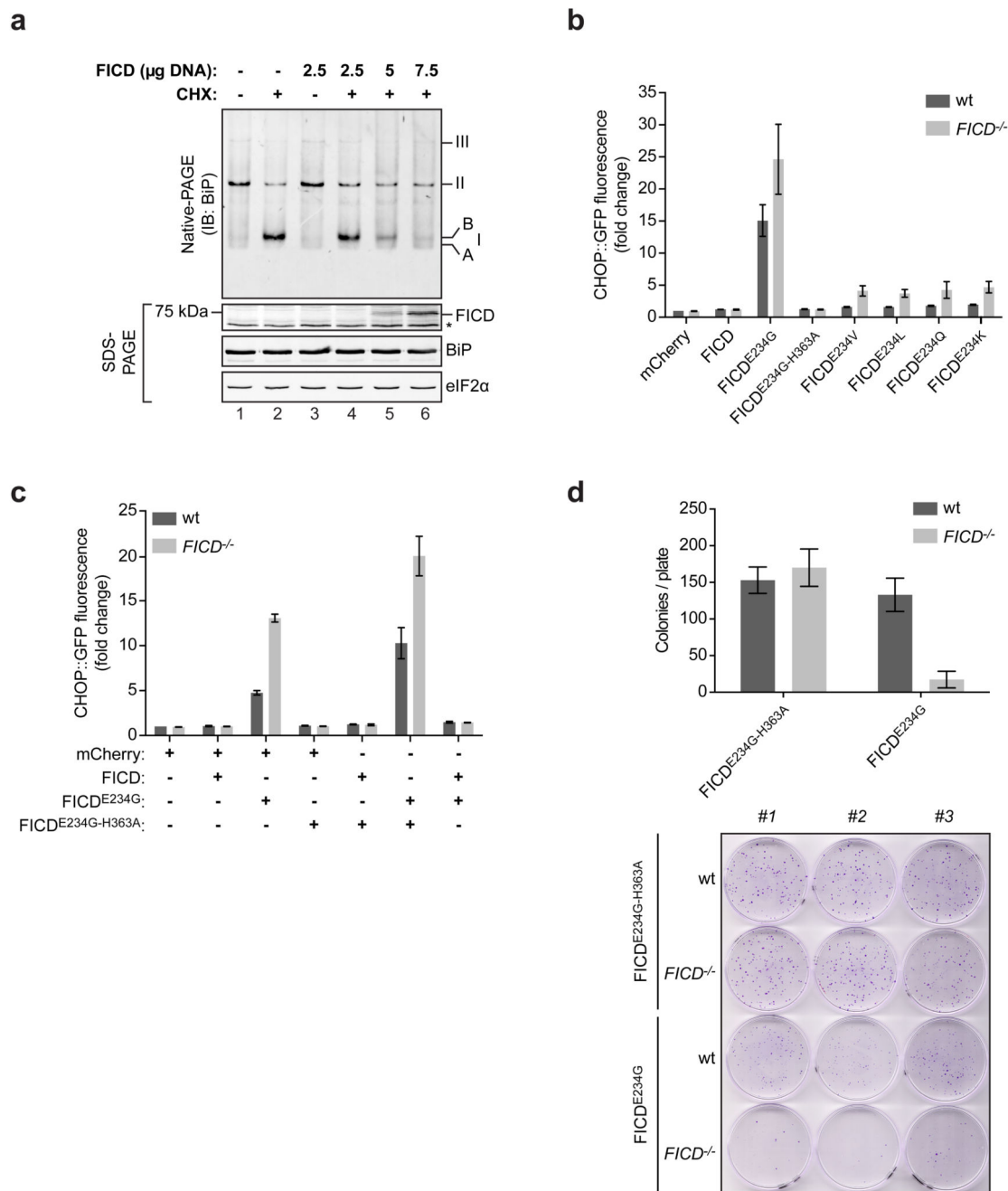
Figure 6. FICD counteracts BiP AMPylation in cells
(**a**) Immunoblot of endogenous BiP from CHO-K1 cells transfected with the indicated amount of plasmid DNA encoding wildtype FICD and exposed to cycloheximide (CHX) resolved by native-PAGE. The AMPylated 'B' form of BiP is indicated (as are the other major species, see Fig. 1 legend). Immunoblots of the same samples resolved by SDS-PAGE report on FICD, total BiP and total eIF2α (which also serves as a loading control). The asterisk indicates a background band. Data representative of three independent experiments are shown.

(**b**) Activity of an integrated *CHOP::GFP* UPR reporter in isogenic wildtype and FICD-deficient CHO-K1 cells following transfection with plasmids encoding the indicated FICD derivatives and an mCherry transfection marker). Shown are the median values ± SD of the GFP fluorescent signal of the mCherry-positive cells from three independent experiments (fold change relative to wildtype cells transfected with control plasmid DNA encoding mCherry only).

(**c**) As in "b", but cells were co-transfected with the indicated pairs of plasmids. Data from three independent experiments are shown.

(**d**) Bar diagram of puromycin-resistant colonies of wildtype and FICD-deficient CHO-K1 cells transduced with a puromycin resistance marked retrovirus expressing a catalytically inactive FICD$^{E234G-H363A}$ or de-AMPylation defective/AMPylation active FICD^{E234G}. Shown are the mean values ± SD of the number of colonies per plate from three replicates. Below is a photograph of the crystal violet stained colonies from the samples described above.

Uncropped blot images are shown in Supplementary Data Set 1.
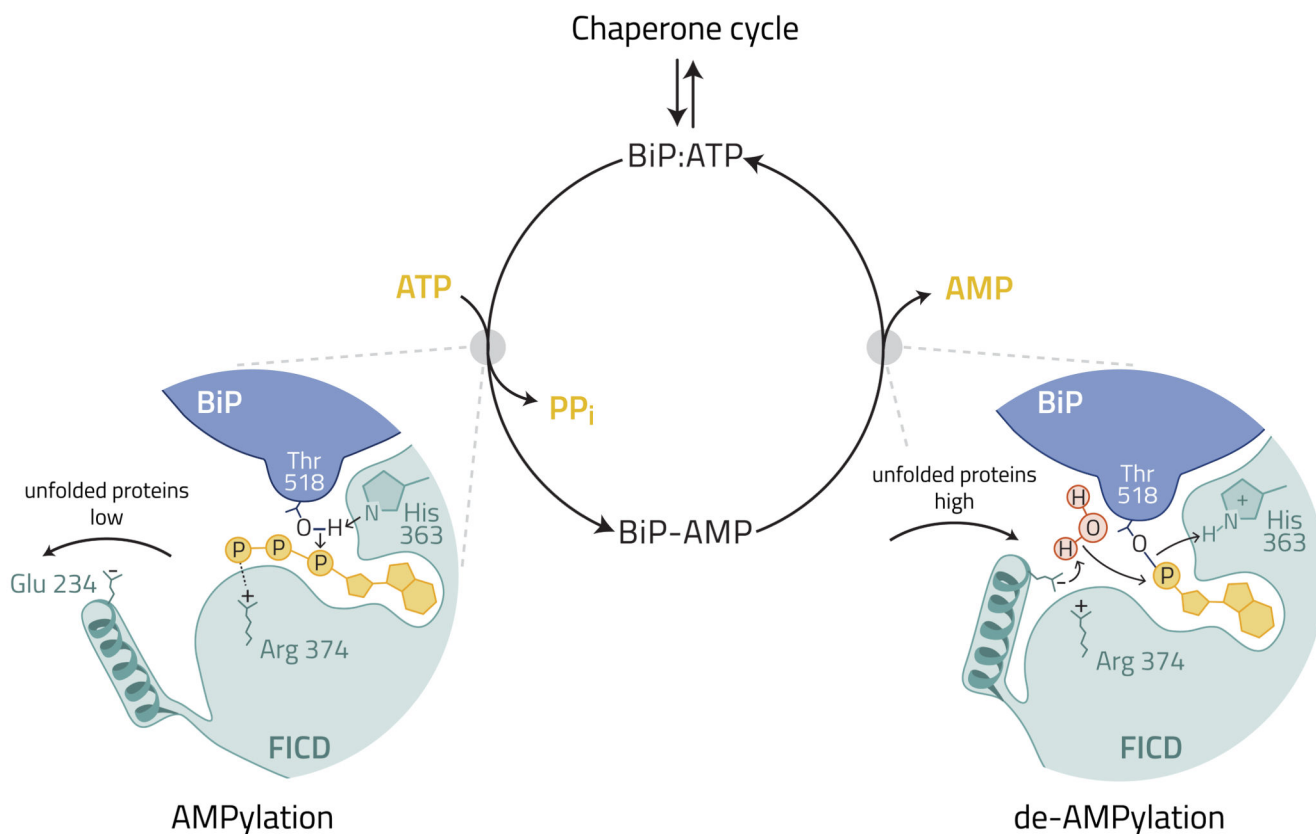
Figure 7. A hypothetical model depicting regulation of the FICD-mediated BiP AMPylation and de-AMPylation cycle by the disposition of E234

A cellular mechanism responsive to the changes in unfolded protein load is hypothesized to switch FICD's function by altering the position of E234.

When unfolded proteins are scarce, active disengagement of FICD's E234 promotes the AMPylation-competent alignment of T518 of BiP, ATP and key residues from the active site (H363 and R374) 16,17, inactivating BiP. When unfolded proteins are abundant FICD returns to its default state. The engaged E234 of FICD coordinates a water molecule to attack the phosphodiester bond between AMP and T518 of BiP. The essential role of FICD's H363 in de-AMPylation is plausibly attributed to protonation of the BiP T518 leaving group. De-AMPylation returns BiP to the chaperone cycle. The bold arrows indicate a hypothesized movement of the regulatory α-helix harboring E234 to switch FICD's catalytic activities and the light arrows indicate the hypothetical flow of electrons according to the proposed catalytic mechanism.